A Low Mass Translation Mechanism for Planetary FTIR Spectrometry using an Ultrasonic Piezo Linear Motor

Matthew Heverly*, Sean Dougherty*, Geoffrey Toon**, Alejandro Soto**, Jean-Francois Blavier**

Abstract

One of the key components of a Fourier Transform Infrared Spectrometer (FTIR) is the linear translation stage used to vary the optical path length between the two arms of the interferometer. This translation mechanism must produce extremely constant velocity motion across its entire range of travel to allow the instrument to attain high signal-to-noise ratio and spectral resolving power. A new spectrometer is being developed at the Jet Propulsion Laboratory under NASA's Planetary Instrument Definition and Development Program (PIDDP). The goal of this project is to build upon existing spaceborne FTIR spectrometer technology to produce a new instrument prototype that has drastically superior spectral resolution and substantially lower mass, making it feasible for planetary exploration. In order to achieve these goals, Alliance Spacesystems, Inc. (ASI) has developed a linear translation mechanism using a novel ultrasonic piezo linear motor in conjunction with a fully kinematic, fault tolerant linear rail system. The piezo motor provides extremely smooth motion, is inherently redundant, and is capable of producing unlimited travel. The kinematic rail uses spherical Vespel® rollers and bushings, which eliminates the need for wet lubrication, while providing a fault tolerant platform for smooth linear motion that will not bind under misalignment or structural deformation. This system can produce velocities from 10 – 100 mm/s with less than 1% velocity error over the entire 100-mm length of travel for a total mechanism mass of less than 850 grams. This system has performed over half a million strokes under vacuum without excessive wear or degradation in performance. This paper covers the design, development, and testing of this linear translation mechanism as part of the Planetary Atmosphere Occultation Spectrometer (PAOS) instrument prototype development program.

Introduction and Background

The Planetary Atmosphere Occultation Spectrometer uses the solar occultation technique to search for trace gases in a planetary atmosphere. The instrument, a Fourier Transform Spectrometer (FTS), views the sun through a planet's atmosphere at sunrise and sunset. As the sunlight passes through the planet's limb, the gasses in the atmosphere selectively absorb certain wavelengths of light. The instrument measures the flux of the incident light at different wavelengths and is able to quantify the atmospheric composition as a function of altitude from the depths of the various absorption lines. Since the sun is a very bright radiation source, these occultation spectra can be of very high spectral resolution and signal-to-noise ratio, providing ultra-high sensitivity to trace gases in the planetary atmosphere under study.

At the heart of any FTS is a Michelson interferometer, which splits the incoming radiation and sends it down two arms with different path lengths. When the two beams recombine interference occurs. By varying the optical path length difference between the two arms of the interferometer, the incoming light is interferometrically modulated. The different wavelengths present in the radiation are modulated at different frequencies. So applying a Fourier transform to the interferogram produces a spectrum of light absorption levels vs. wavelength and reveals the composition of the observed atmosphere. The spectral resolution of an FTS is a function of the maximum optical path difference (OPD), and the quality of the spectra is critically dependant upon the uniformity of the moving cube corner's motion. An example spectrum for the atmosphere of Saturn's moon Titan is shown in Figure 1.

---

* Alliance Spacesystems, Inc., Pasadena, CA
** Jet Propulsion Laboratory, California Institute of Technology, Pasadena, CA

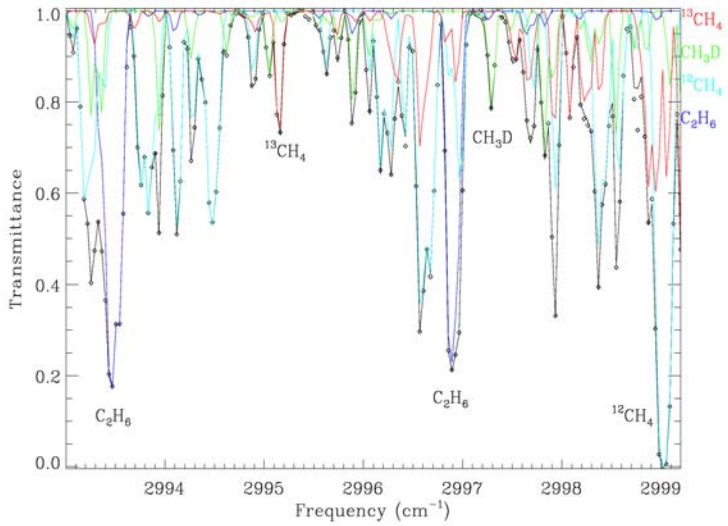

Figure 1. Simulated limb transmittance spectrum (0.05 cm^{-1} spectral resolution) at 300 km tangent altitude in the atmosphere of Titan, showing the absorption contributions of ethane and various isotopomers of methane. This 6 cm^{-1} interval represents less than 0.2% of the full PAOS bandpass

Most spaceborne, high-resolution Fourier transform spectrometers to date have been Earth-orbiting instruments constructed using traditional electromagnetic actuators in the form of direct drive voice coils or brushless DC motors with lead screws or belt drive systems to drive the translation stage (Persky, 1995). These mechanisms are either too massive or don't have the requisite spectral resolution for future exploration of planetary atmospheres. Figure 2 below shows a comparison of the PAOS instrument requirements with other Fourier Transform Spectrometers by plotting the overall instrument mass versus the number of spectral channels (simultaneous spectral bandwidth divided by spectral resolution) (Toon, 2001).

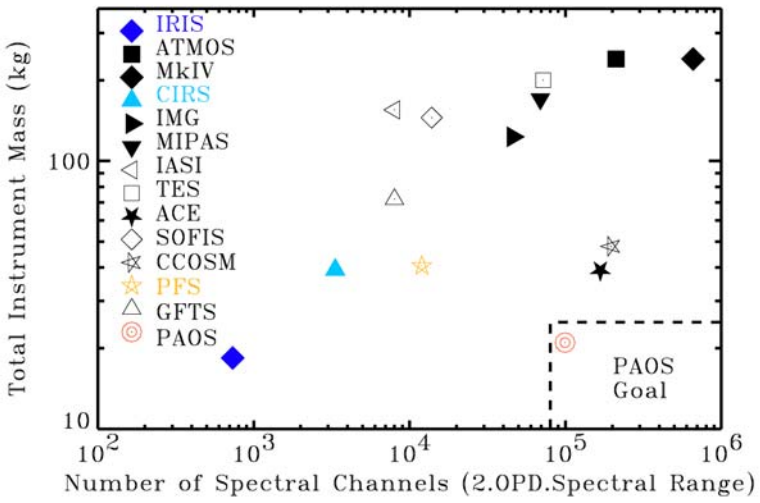

Figure 2. Comparison of PAOS mass and spectral resolving power with other FTS. Colored symbols represent planetary instruments. Filled symbols represent launched instruments.

Prototype Mechanism

The PAOS instrument will incorporate new technology in several different areas. It will use new laser diodes for the reference laser and new electronics for on-board data processing and compression. The subsystem with the lowest technology readiness level at the time of the PIDDP proposal, however, was the translation mechanism and thus it has been the focus of the PIDDP effort up to the time of this publication. The mechanism is required to move a 125-gram cube corner retro-reflector through a 100 mm stroke at a constant velocity of 30 mm/s with less than 1% error in velocity (± 0.15 mm/s rms) over a life of one million strokes. The goal of the development was to make a mechanism that could accomplish all these requirements while packaged as small as possible, consuming less than 5 watts of power on average and having a mass less than 4 kg. Because this is an interferometer, it is sensitive to motions as small as a few nanometers and can sense disturbances into the megahertz range.

In modern FTSs, the effects of velocity errors are removed, to first order, by means of a reference laser that traverses the same optical path as the infrared radiation of interest. The laser is used to trigger the sampling of the infrared interferograms, ensuring that they are at equal increments of optical delay. But due to the fact that the laser beam hits different parts of the optics from the IR beam, and the fact that the laser is at a different frequency, there still remain significant second-order effects that arise from velocity non-uniformities. Since these second and third order disturbances are very hard to model analytically, our development approach was to build several prototypes and test them as early as possible. Once tested, the performance of the mechanism could be characterized and the causes of velocity jitter could be better understood. Several different concepts including voice coils, lead screws, linkages, and belt drive systems were tested. Off the shelf mechanisms as well as quick, custom prototypes were built and evaluated. This helped to reduce the time involved in the development process while still providing valuable data about the root causes of velocity error. The lessons learned during each of these tests were then folded back into the next iteration of the design cycle to continually improve the mechanism performance and robustness.

The final prototype mechanism, shown in Figure 3, uses an ultrasonic piezo motor to move the sled that carries the moving hollow cube-corner retro-reflector (HCCRR). The sled is guided by a kinematic rail system that uses three spherical Vespel rollers along with the preload of the piezo motor to fully constrain the cube corner sled's motion. The sled is moved through the required 100 mm stroke and follows a trapezoidal motion profile spending 85% of its duty cycle at the target speed of 30 mm/s. The second cube corner, required for the interferometer, is held stationary and is attached to a common base plate. A top view of the mechanism is shown in Figures 4 and 5 with the moving sled at its left and right ends of travel positions respectively.

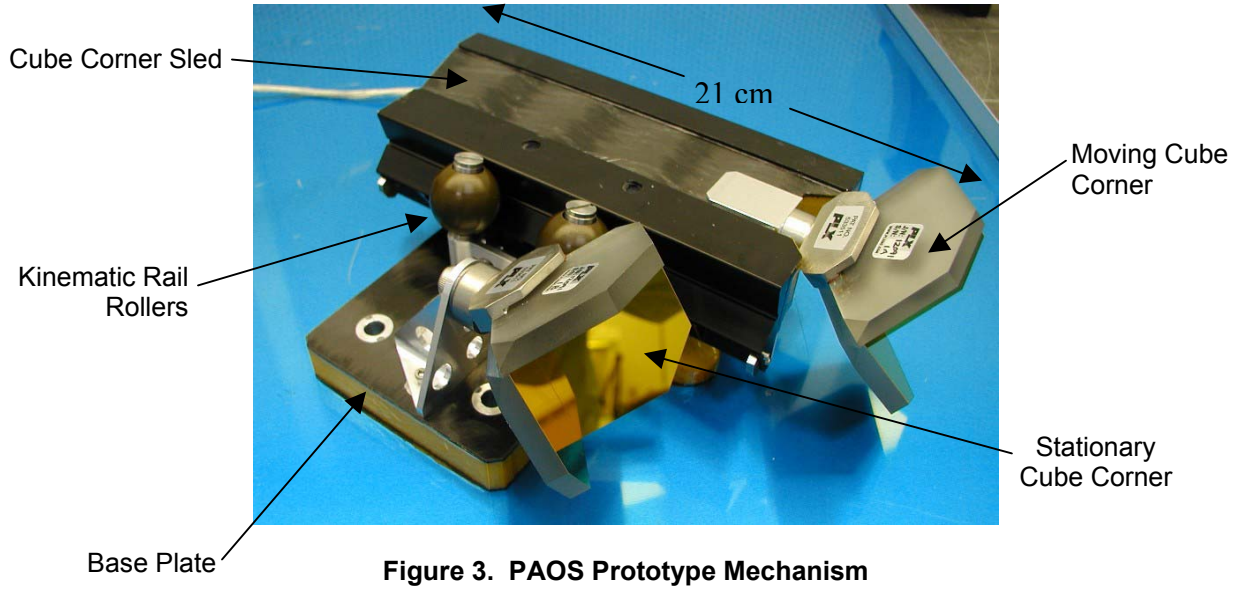

Figure 3. PAOS Prototype Mechanism

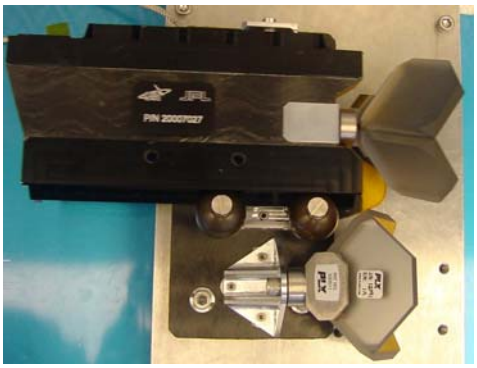

Figure 4. Left End of Travel

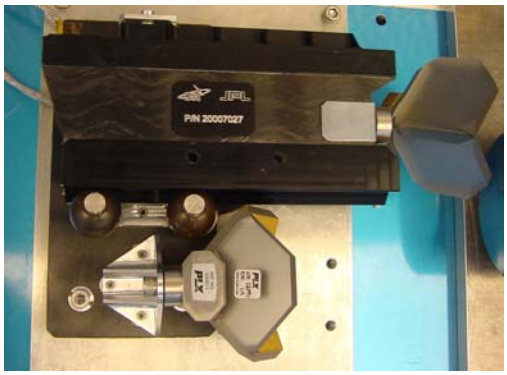

Figure 5. Right End of Travel

Linear Piezo Motor

Ultimately the design goals and the developmental nature of the project led to the decision to use new technology in the form of an ultrasonic linear piezo motor developed by Nanomotion Ltd, Figure 6. This motor allows for drastic mass savings over more traditional systems while, at the same time, producing very constant velocity motion. Piezoelectric materials allow mechanical strain to be directly coupled to electrical potential. The motor works by simultaneously exciting both a longitudinal (Figure 7) and transverse (Figure 8) bending mode in a piezo element using two sinusoidal voltage inputs. The result of these combined modes is an elliptical motion at the tip of the piezo element that drives a linear stage through a preloaded friction interface.

Figure 6. HR-4 (Four Element) Linear Piezo

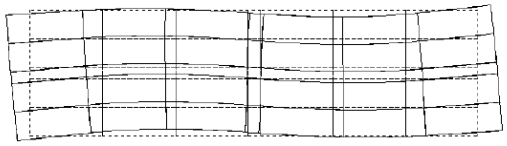

Figure 7. Longitudinal Extension Mode

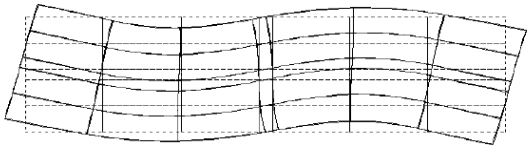

Figure 8. Transverse Bending Mode

The piezo elements have a hard ceramic alumina finger tip attached to the element body, which interacts with an alumina strip mounted to the mechanism's moving sled as shown in Figure 9. This provides an optimum coefficient of friction and significantly reduces wear. During extension and bending of the piezo element the sled is actively forced in the desired direction, while during contraction and bending in the other direction, the piezo either slides on, or separates slightly from the ceramic drive strip. This motion results in a net forward movement of the sled over one cycle of the piezo element. This elliptical motion takes place at a frequency of 40 kHz. Because of the speed of this oscillation, the mass of the moving object mechanically filters any jitter, resulting in extremely smooth linear motion. The magnitude of the displacement during any one cycle is proportional to the voltage applied across the piezo element. This voltage can be changed rapidly to control the velocity of the moving sled. Since the piezo element displacements are on the nanometer scale, these motors can also be used to achieve positional accuracies of less than 10 nanometers. A standard servo controller with any standard feedback device can close the control loop and servo the applied voltage in order to follow a desired trajectory profile.

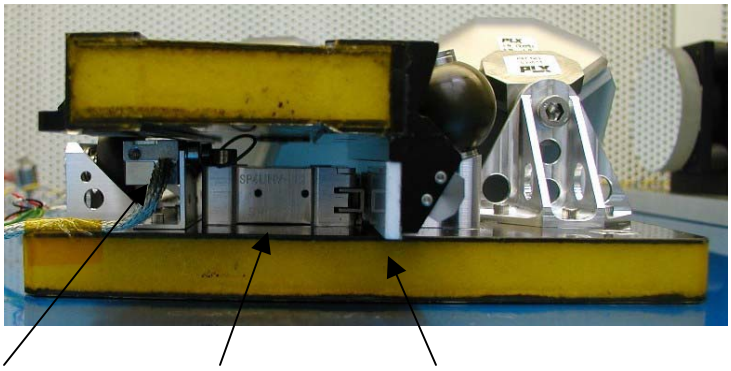

Figure 9. PAOS Mechanism Rear View

The piezo elements can be stacked side by side and operated in parallel to give a proportional increase in driving force. This also introduces redundancy such that if one element fails, it simply results in a decrease in available force rather than catastrophic failure (Uniformity of velocity in this configuration is yet to be quantified). The current prototype uses a vacuum-rated, four-fingered piezo motor with a mass of 73 grams. It is able to provide approximately 4 pounds of force in the driving direction. This allows ample margin for driving the mechanism in any orientation (including vertically against gravity), which allows for versatility in earth testing.

A factor in the decision of whether or not to use piezo motors for this development was their lack of flight heritage. It was decided that although these motors have never flown on a space flight mission, they possessed all the necessary qualities for a flight mechanism and offered such dramatic benefits that they could not be overlooked. Given the research and development nature of the PIDDP program, the piezo motors were incorporated into the design. Piezoelectric materials have been flown in the past on projects such as the Large Angle and Spectrometric Coronagraph (LASCO) telescope aboard the Solar and Heliospheric Observatory (SOHO) spacecraft, but have primarily been used as a stack of piezo wafers with an applied DC voltage to give highly accurate, but extremely small deflections, in the μm range (Burger, 1995). The ultrasonic piezo motor uses the same materials, but employs an AC voltage to excite the natural frequency of the piezoelectric element to create motion. These motors have been used for several years in vacuum environments for applications such as scanning electron microscopes and are available in vacuum-rated versions rated down to 10^{-10} torr. Nanomotion Ltd. has conducted thermal testing, proving a survivability temperature as low as –120 deg C and an operational range of –55 deg C to +85 deg C. A 4.6 million-cycle vacuum life test has also been run showing no degradation in motor performance over the life of the eighty-day test. Outgassing tests performed per ASTM E 595-93 standard have shown a total mass loss (TML) of 0.60% and less than 0.018% collected volatile condensable materials (CVCM) under vacuum conditions, which exceeds the recommended TML $<$ 1.0% and CVCM $<$ 0.1%. ASI is currently working to fully qualify these motors for space flight applications. The development of this motor as an alternative to traditional motors looks very promising, as the most substantial issues have already been addressed in the construction of these motors for terrestrial vacuum applications.

Rail Design

Several rail systems were tested in the early stages of the program including recirculating linear ball bearings, crossed roller bearings, as well as flexure and linkage systems. With all systems that used recirculating balls, the impact of the ball bearings striking the guiding rod was evident in the velocity error (whose measurement is described later). The prototypes that used crossed roller bearings all performed well, but the crossed rollers have issues that make them less desirable for space mechanisms. Linear crossed roller bearings require a caging system to separate and equally space the cylindrical rollers. Over time the cage can migrate to one end of travel. This will lead to the cage striking one end of the rail system and gradually reducing the range of travel, which will eventually lead to a mechanism failure. This is not generally a concern in terrestrial applications because the cage can easily be reset by hand, but for

a flight mechanism, additional design elements must be introduced to mitigate this problem (Roberts, 1994). A crossed roller bearing is also inherently over-constrained and depends upon tight machining tolerances to prevent the system from binding. A slight misalignment or small change in preload (due to thermal expansion for example) can produce a drastic increase in the force required to move the sled, which could cause binding.

After investigating the pros and cons of various designs, a rail system was developed that uses the preload of the piezo motor in conjunction with three spherical rollers to create a fully kinematic rail system that guides the moving corner cube sled. Figure 10 shows a two-dimensional schematic of the rail configuration. A spherical roller (furthest right in the figure) is attached to the base structure. The sled has an integral V-groove that rides on the spherical roller, resulting in two contact points. A separate spherical roller (furthest left in the figure) is also attached to the base structure and creates another point contact on a flat surface on the moving sled. The piezo motor is preloaded against the moving sled producing a force that results in a moment around the V-groove roller that is reacted by the single roller, resulting in a fully kinematic design.

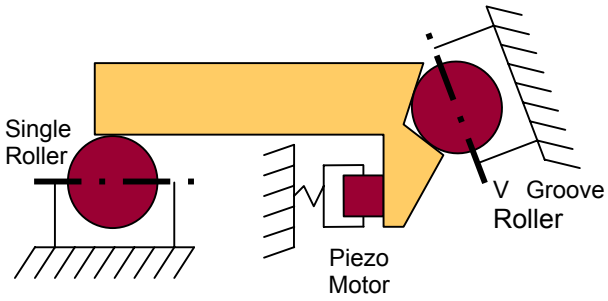

Figure 10. 2-D Kinematic Rail Schematic

The rail design can be expanded to three dimensions by adding a second V-groove roller (shown in Figure 11). If the single roller and piezo motor preload force act between the two v-groove rollers, the rail system becomes kinematic in three dimensions, leaving the translation of the sled as the only remaining degree of freedom. Since the rail system is kinematic, the force required to move the sled should not change if small misalignments are introduced due to thermal distortion of the structure. The design also helps to reduce the need for tight machining tolerances in order to align the system properly.

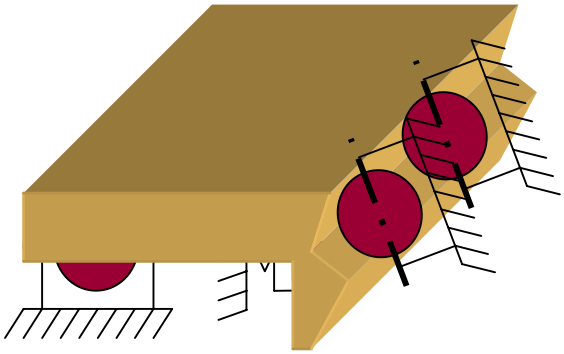

Figure 11. 3-D Kinematic Rail Schematic

All three of the spherical rollers are made from Vespel SP3. Initially, a pair of preloaded radial ball bearings was used inside each of the spherical rollers, yielding good velocity uniformity performance. Tests were then run without the ball bearings using only the Vespel rollers as bushings, sliding on steel pins coated with Dicronite® dry film lubricant as shown in Figure 12. These tests yielded similar results to the tests using bearings, but without the requirement for wet lubrication. This is advantageous because the lubrication under vacuum conditions could outgas and contaminate the optical surfaces. With the rollers acting as bushings the force necessary to move the mechanism is proportional to the preload of the piezo motor and the coefficient of friction between the sliding Vespel/Dicronite interface. Under normal ambient conditions the mechanism requires approximately 4 N of force to move the sled. Under vacuum conditions, the coefficient of friction for Vespel SP3 reduces by a factor of 10 due to the removal of moisture on the contacting surfaces. This further reduces the power required by the system and increases the motor's force margin over stall conditions.

The V-groove and flat track of the sled are hard anodized aluminum with a surface finish of 8, giving a hard, smooth surface for the rollers to contact. And even if the rollers were to bind on the steel pins, they are still able to slide on the anodized aluminum tracks. This makes the system single fault tolerant. Tests

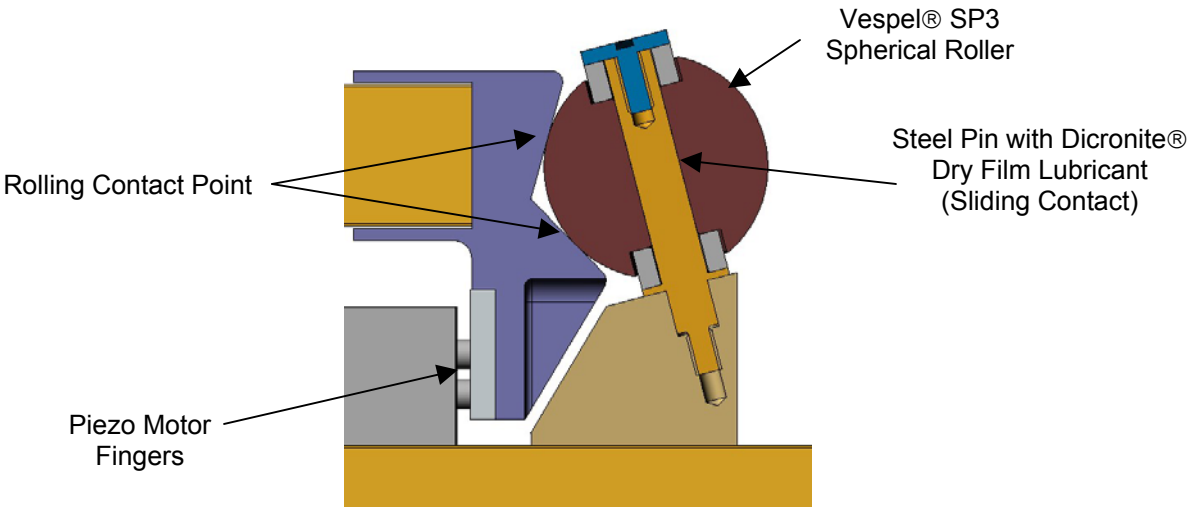

Figure 12. Spherical Roller Cross Section

were performed in this condition, resulting in only a slight increase in the required force and no compromise in velocity smoothness.

Design Details

Unpowered Holding Force

The piezo motor moves the output stage through an oscillation of the piezo fingers through a friction interface. When the motor is not powered, the piezo fingers are still preloaded against the moving sled. This static interface between the piezo fingers and the sled gives the benefit of unpowered holding force. Under ambient conditions the current prototype has a holding force of approximately 13 N, which is directly proportional to the preload of the fingers and the number of elements used in the motor. The mechanism can however, be readily backdriven by simply overcoming the frictional holding force without any damage to the motor or friction interface. This holding force is likely not enough to cage the mechanism for launch conditions, but will hold the mechanism during orbital maneuvers of the spacecraft after the launch lock mechanism has been released.

Mechanical Hardstops

Two mechanical hardstops are incorporated into the mechanism, one at either end of travel. These hardstops protect the mechanism and the optics from overtravel, but also allow for positional calibration of the mechanism at startup. Since the piezo fingers slip on the ceramic drive strip when the stall force of the motor is exceeded, there is no damage done to the mechanism when the moving sled encounters a hardstop. To calibrate the mechanism it is driven in one direction until a position error threshold is exceeded. The position tracking software is then re-zeroed to create a home position in the controller, which eliminates the need for an absolute feedback device.

Power Consumption

The four-element piezo motor itself consumes approximately 3.25 watts of power under normal operating conditions on Earth. Power consumption will be slightly reduced (although exactly how much has yet to be quantified) on orbit due to the decrease in the coefficient of friction of the Vespel rollers in vacuum and the corresponding reduction in the force necessary to move the cube corner sled. The drive electronics used in the prototype are not designed for efficiency as they are for industrial applications, and consume approximately 4 watts giving a total of 7.25 watts total power consumption for the mechanism. The piezo elements require a sinusoidal voltage of 120 volts for excitation. The control electronics currently run off of a 24 or 48 volt DC bus and a majority of the drive electronics' power consumption is used for voltage conversion.

Feedback and Control

The prototype currently uses a vacuum rated, Renishaw 0.1-micron linear encoder for positional feedback to control the velocity profile. A standard servo controller running a cascaded velocity/position control loop is used to control the motion profile. The interferometer's reference laser will eventually replace the encoder as the mechanism's feedback device. The zero crossings of the sinusoidal laser interference pattern can be counted in much the same was as a traditional encoder allowing a standard controller to be implemented. Using the laser as feedback should increase the robustness of the mechanism by decreasing the number of subsystems. It is also expected that this will increase the performance of the mechanisms due to the high resolution of the laser interferometer and the fact that the control system will feedback directly on the optical path difference, which is the variable of interest.

Testing

The prototype mechanism was tested using the double pass interferometer setup shown in Figure 13 to give true output velocity measurements. A 633-nm wavelength single-frequency He:Ne reference laser is sent through a beam splitter with one half of the beam going to the stationary cube corner and the other half of the beam going to the moving cube corner. The beams reflect off the cube corners onto the retro reflector where the beams then retrace their paths. The two beams then recombine at the beam splitter where their overlapping waves add and subtract, depending on their relative path difference, to produce an interference pattern. If the moving cube corner translates at a constant velocity, the interference pattern is a constant frequency sine wave. The waveform pattern in the detector is sampled at 1MHz and the data is analyzed using a custom analysis tool built by ASI.

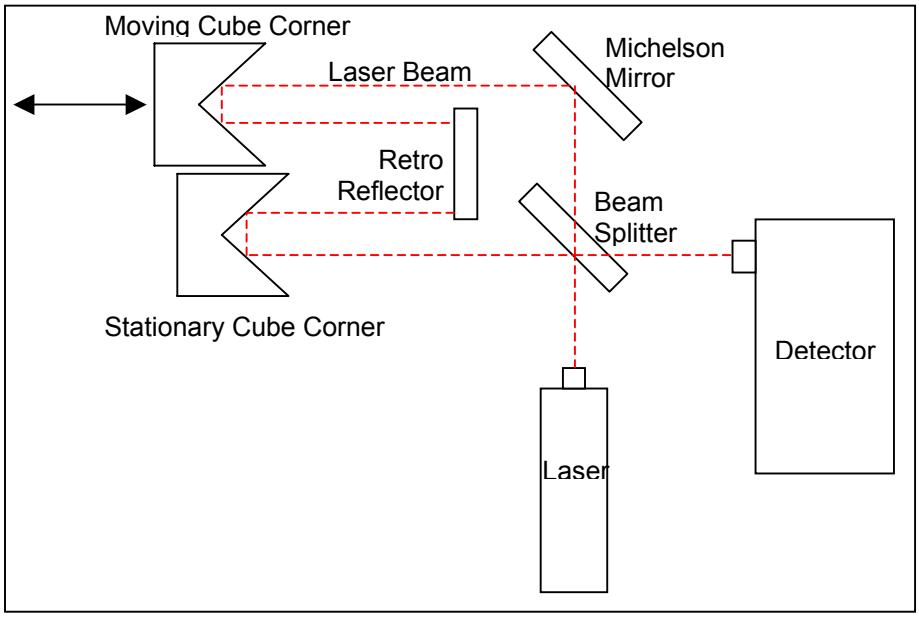

Figure 13. Laser Interferometer Test Setup

Figure 14 shows the original laser intensity depicted in the form of a sine wave. The Hilbert transform of this data is then taken to calculate the frequency of the data at every point. This frequency is directly proportional to the cube corner linear velocity. The calculated velocity is plotted in Figure 15. The Fourier transform can then be taken of the velocity data to identify the frequencies at which disturbances occur and their magnitude. This velocity error data is shown in Figure 16. Using this method, the true velocity error of the cube corner can be measured and the frequency of the disturbances can be quantified, which helps to identify and eliminate the sources of velocity error.

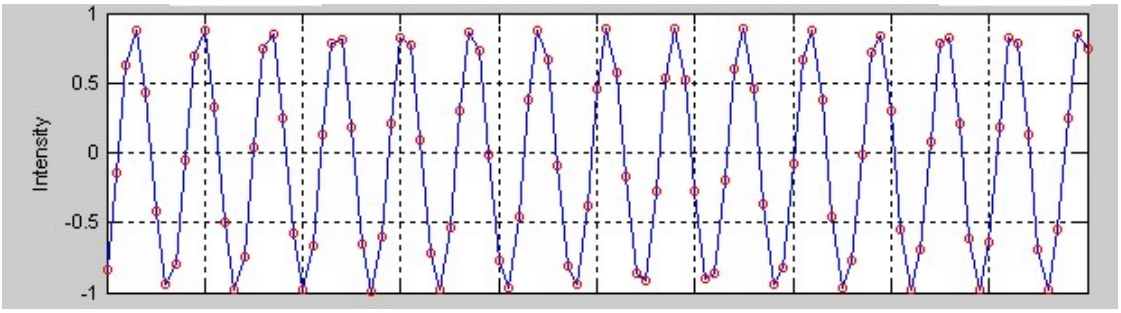

Figure 14. Original laser intensity data over 0.1 ms sample period (red circles are sample points)

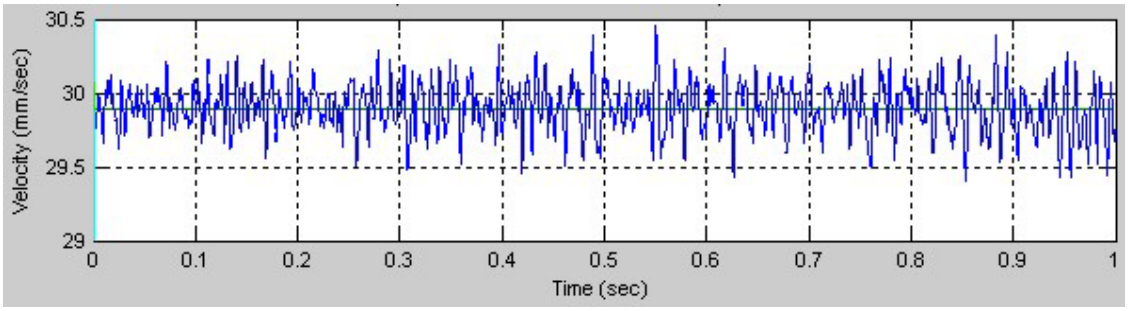

Figure 15. Calculated velocity (frequency) vs. time over 1 second sample period

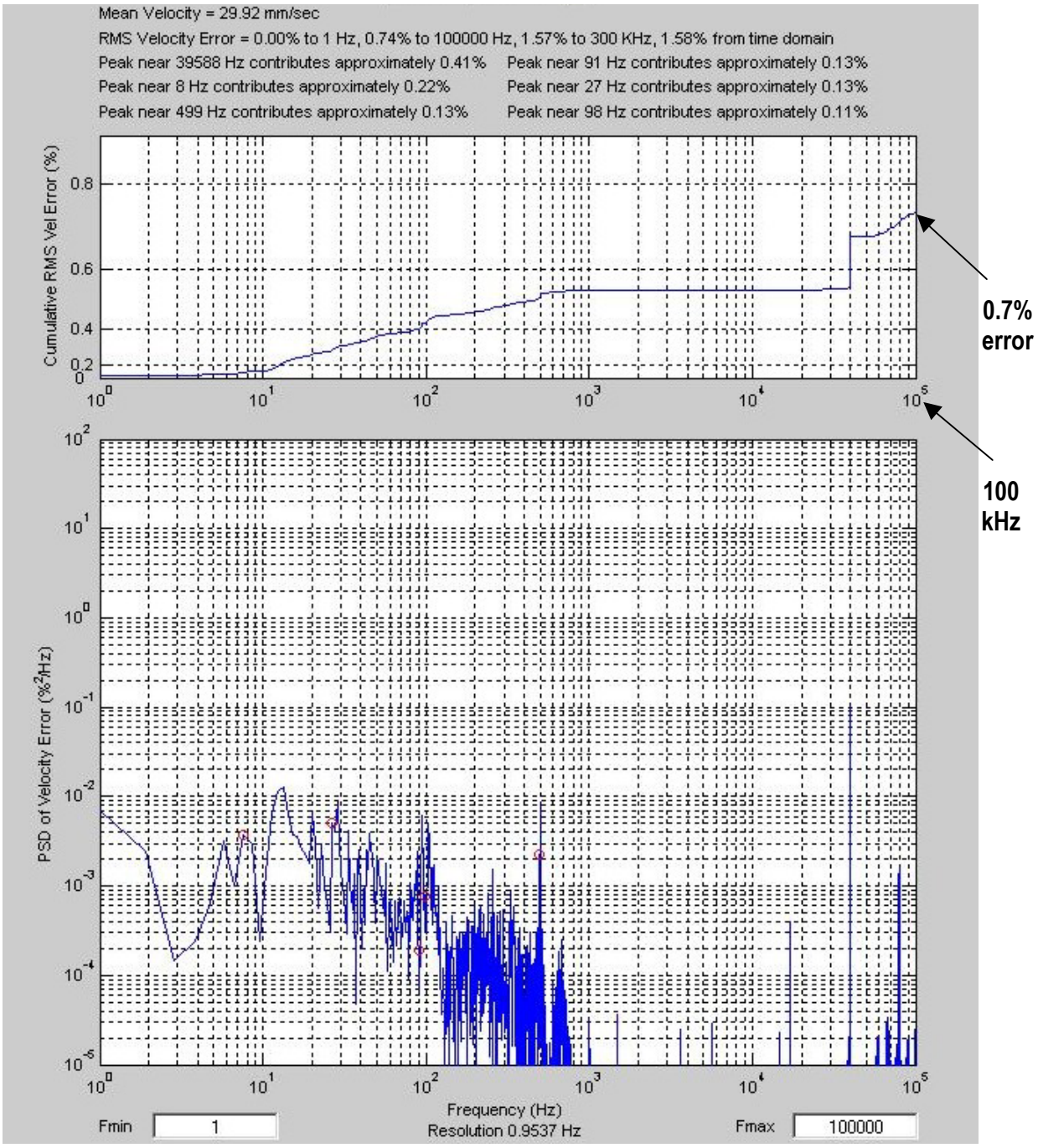

Figure 16. Velocity Error Data for the PAOS Mechanism

Over 500 runs have been conducted using the current prototype, characterizing its performance and robustness. The mechanism is consistantly able to produce less than 0.7% cumulative velocity error at frequencies up to 100 kHz. It is anticipated that using the reference laser as feedback will further improve this error by rejecting low frequency disturbances that are within the servo range of the control system.

Future Work

At the time of this writing, a life test of the mechanism had been started. The test is an ambient condition life test in which the mechanism will run continuously for one month, resulting in 300,000 full cycles of the mechanism at the nominal speed of 30 mm/s. This test will characterize wear at the interface between the piezo motor fingers and the ceramic strip, in the Vespel rollers sliding against the steel pins, and the rolling contact between the Vespel rollers and the hard-anodized aluminum sled. The test will also characterize any change in the force required to move the mechanism, positional error along the velocity profile, and velocity error over the life test. A second life test will then be conducted for a two-week period in a vacuum chamber. This test will characterize the mechanism's performance as well as heat dissipation under vacuum conditions.

It is planned that the next design iteration will incorporate a locking device to protect the mechanism during launch vibrations. It will also incorporate all of the optics on a single structure and use the interferometer reference laser as the primary feedback device.

Work to qualify the piezo motor for space flight applications will continue. Further thermal-vacuum testing will be conducted to better characterize the properties of the motor under these conditions, as well as characterize the heat dissipation. Vibration testing will be conducted to better understand how the motors will react to launch load environments. The drive electronics will also be re-designed and qualified for space flight. Once these motors are qualified they can easily be incorporated into a new mechanism design without the need to re-qualify the motor at the piece part level. The motor is a stand-alone component that can be integrated into a system to quickly and cost effectively create a linear or rotary mechanism.

Lessons Learned

In order to reduce the mass as much as possible in the current design, the piezo motor was used to preload the kinematic rail system. While this eliminated the need for a fourth roller and reduced the overall system mass, it also reduced the stiffness of the system. Each of the piezo elements are preloaded against the ceramic strip with independent springs that are soft when compared to the rest of the system. This reduces the natural frequency of the system and, in turn, reduces the margin of stability in the control loop. In future designs an independent roller will be used to preload the rails, and the line of action of the preload force from the piezo fingers will act directly through the center of the dual spherical rollers. This will allow the mechanism to have an adjustable preload independent of the fixed preload in the piezo motor fingers.

The use of the piezo motor to preload the system also precluded testing of the rails and motor individually. The drag force of the rail system alone could not be directly measured due to the necessity of the piezo motor to complete the system and the associated friction holding force. While combining functionality of key components saves packaging space and mass, it makes individual component performance characterization difficult. The addition of independent preload rollers in the next design will slightly increase the mechanisms size but it will provide the ability to better characterize the performance of the rail system at the sub-assembly level and understand its contribution to the overall mechanism performance.

The ability to quickly build prototypes and conduct tests was invaluable for this type of development project. When dealing with such stringent requirements, new technology, and complex systems, there is no substitute for testing the actual hardware. During the course of the prototype development, more than ten mechanisms were built and tested using the interferometer setup. This gave a tremendous amount of insight into the causes of velocity error over a broad frequency range. Inevitably things that are not accounted for in the design will show up in testing, and the sooner the mechanism can be tested, the sooner design iterations can be incorporated into the next hardware design.

Having custom data reduction software to quickly quantify and visually characterize the results of performance testing saved a tremendous amount of time during the actual testing of the mechanisms.

Nearly 1,500 total runs on different mechanisms were conducted over a six month period of time. Having a software tool that collected, analyzed, and displayed data real time made it practical to change one variable at a time in order to clearly understand how that variable affected the mechanism. It also made it easy to collect a number of samples and verify that the results were consistent and not a product of a transient phenomenon.

Early testing revealed a sharp velocity disturbance at an input frequency of 40 kHz, which was quickly dismissed as electrical noise in the data acquisition due to the sinusoidal voltage used to excite the piezo elements. After further testing and unsuccessful attempts to eliminate the error with electrical shielding it was revealed that the disturbance is actually mechanical vibration and not simply electrical noise. This vibration can be filtered mechanically using springs in the cube corner mounts but careful consideration must be given to this input when dealing with mechanisms that are sensitive to disturbances over such a wide frequency range.

Conclusions

A new linear translation mechanism has been developed that will allow the PAOS instrument to offer improved performance and lower mass compared to existing spaceborne spectrometers. The low mass (< 1 kg) of this mechanism is a direct result of the enabling technology represented by the ultrasonic piezo motor. These motors provide a new alternative for linear space mechanisms and offer smooth, precise motion, inherent redundancy, low mass, and simplified integration. The kinematic Vespel rail system provides a solution that is fault tolerant and insensitive to structural misalignments due to thermal distortion or manufacturing tolerances. The design can easily be adapted to provide any stroke length over a wide range of velocities. Initial testing shows consistent velocity error of less than 0.7% in a mechanism that requires no wet lubrication and is small enough to hold in a single hand.

Acknowledgements

We acknowledge funding from the NASA Planetary Instrument Design and Definition Program. Part of this research was performed at the Jet Propulsion Laboratory under contract with NASA. We also acknowledge the extensive assistance provided by Nanomotion Ltd. in the evaluation and implementation of the piezo motors and drives.

References

Karasikov, Dr. Nir (2000). *A Novel Non-Magnetic Miniature Motor for Ultra High Vacuum Applications*, paper for Nanomotion Ltd.

Persky, M.J. *A Review of Spaceborne Infrared Fourier Transform Spectrometers for Remote Sensing*, presented at The American Institute of Physics, October 1995.
Roberts, E.W., et al. *Development of Long-Life, Low-Noise Linear Bearings for Atmospheric Interferometry*, paper presented at the 34th Aerospace Mechanisms Symposium on May18-20, 1994.
Toon, Dr. G.C., et al (2001). *Planetary Atmosphere Occultation Spectrometer: A Miniature High Resolution Fourier Transform Infrared Spectrometer*, proposal for Jet Propulsion Laboratory.

Burger, F., Eder, J. *High Precision Pointing Device for the LASCO instrument on SOHO*, paper presented at the 6th European Space Mechanisms & Tribology Symposium on October 4-6, 1995.